

Facile synthesis of single crystalline SnO₂ nanowires

Zongying Cai^{a,b,*}, Junshou Li^b

^a*Metallurgical & Energy Engineering, Hebei United University, Tangshan, Hebei 063009, PR China*

^b*Institute of Advanced Materials, Mechanical Engineering College, Shijiazhuang, Hebei 050003, PR China*

Received 8 May 2012; received in revised form 12 June 2012; accepted 12 June 2012

Available online 18 June 2012

Abstract

Single crystalline SnO₂ nanowires with diameter in the range of 10–100 nm and several micrometers in length have been successfully prepared by the combustion technique in air using Al, Cu₂O and SnO as the raw materials. FE–SEM and TEM images showed that the nanowires were single crystalline, growing along the [310] direction. The nanowires' growth mechanism was suggested to follow both VLS and VS mechanisms. The formation of SnO₂ nanowires underwent three steps: tin vapor generation via combustion synthesis, oxidation of the tin vapor and its nucleation and subsequent growth. At the same time, porous Al₂O₃ ceramic and Cu–Sn alloy were obtained during the combustion synthesis process.

© 2012 Elsevier Ltd and Techna Group S.r.l. All rights reserved.

Keywords: Nanowires; SnO₂; Combustion synthesis; SHS

1. Introduction

Solid state sensors are one of the most effective tools for the development of devices used for monitoring and controlling of air quality, detecting trace concentration of toxic and combustible gases in air, medical diagnosis, and optimization of combustion [1–3]. It was found that the charge carrier concentration on the surface of metal-oxide semiconductors changes in accordance with the composition of the surrounding atmosphere [4]. Metal-oxide semiconductors such as SnO₂, TiO₂, ZnO, In₂O₃ and WO₃ are popular materials for solid state sensors because of their high response value, fast response, quick recovery, excellent stability and simplicity in fabrication [5–9]. Design and fabrication of metal-oxide semiconductor sensor materials have become one of the most active research fields in recent years.

Tin dioxide (SnO₂), an n-type semiconductor with a band gap of 3.6 eV at 300 K, has been widely utilized in many fields such as dye-sensitized solar cells [10], gas

sensors for detecting leakage [1–4,9], transparent conducting electrodes [11], catalyst supports and electrochemical modifiers on electrodes, etc [12–15]. Recently, one-dimensional (1D) nanostructures such as nanobelts, nanofibers and nanowires have attracted much attention because of their high ratio of specific surface area and electronic structural changes due to quantum confinement. SnO₂ with 1D nanostructures can be applied as semiconductor sensors with high performance. Up to now, 1D nanostructured SnO₂ has been synthesized successfully by many methods including chemical vapor deposition (CVD) [16], the sol–gel template method [17], hydrothermal synthesis [14], the reaction sintering method [18], the co-precipitation method [19], the molten-salt method [9], etc. Although SnO₂ with 1D nanostructures were synthesized by many methods, there were no reports on synthesis of SnO₂ nanowires by combustion synthesis.

Combustion synthesis or self-propagating high temperature synthesis (SHS) represents a relatively new technique for the synthesis of inorganic materials [20–23]. The process takes advantage of the high exothermicity of reactions associated with the synthesis of highly stable compounds [24,25]. With low energy consumption and short reaction period, combustion synthesis is a facile technique to prepare SnO₂ nanowires, especially for

*Corresponding author at: Hebei United University, Metallurgical & Energy Engineering, Hebei 063009, PR China. Tel.: +86 315 2992155; fax: +86 315 2592155.

E-mail address: czy1106@sina.com (Z. Cai).

large-scale industrial production. In the present study, novel SnO_2 nanowires were prepared by combustion synthesis using Al, SnO and Cu_2O as the starting powders. Based on the experimental results, the possible formation mechanism of SnO_2 nanowires was discussed.

2. Material and methods

Commercial powders of aluminum (Al, 99.5% purity, 100–200 mesh), stannous oxide (SnO , 99.5% purity, 200–300 mesh) and cuprous oxide (Cu_2O , 90.0% purity, 200–300 mesh) were used as the raw materials. The raw powders were mixed with stoichiometry and manually ground in an agate mortar in dry condition. Then the mixed powders were put in a clay–graphite crucible and

placed in a combustion chamber after being dried at 120°C for 2 h.

The self-made experimental apparatus used for the synthesis of the nanowires was shown in Fig. 1(a). The powders of the mixed reactants were ignited in an air atmosphere using an electrically heated Alchrome wire coil in the stainless steel combustion chamber. The reaction was initiated at the top of the reactants and propagated through the whole unburned powders by means of combustion wave movement. The combustion process is shown in Fig. 1(b). Once the combustion mixture was ignited and the igniter turned off, the combustion reaction took place drastically and the reaction temperature reached a relatively high level ($1500^\circ\text{C} < T < 3500^\circ\text{C}$) [23]. The high temperature needed for further synthesis was supplied by the self-sustained exothermic chemical reaction. During the short reaction period, the reactants were transformed into loosed flocculent products, which were sputtered and collected on the collector sieves with different meshes.

The X-ray diffraction (XRD) experiment was carried out on an X-ray diffractometer (MXP21VAHF, Mac Sci., Yokohama, Japan) using $\text{Cu K}\alpha$ radiation to characterize the phase structure and composition. The microstructure and chemical composition of the as-prepared products on the collectors were investigated by using field emission scanning electron microscopy (FE-SEM, JSM-6700F, JEOL, Tokyo, Japan) equipped with energy dispersive X-ray spectroscopy (EDS, INCA, Oxford Instrument, England). Transmission electron microscopy (TEM, JEM-2010, JEOL, Tokyo, Japan) was applied to perform further observations and acquire the selected area electron diffraction (SAED) patterns and high resolution transmission electron microscopy (HRTEM).

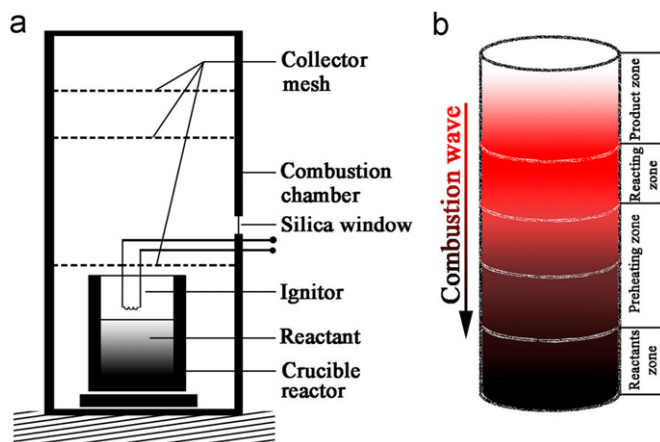


Fig. 1. Schematic diagram of (a) experimental apparatus and (b) combustion process for SHS.

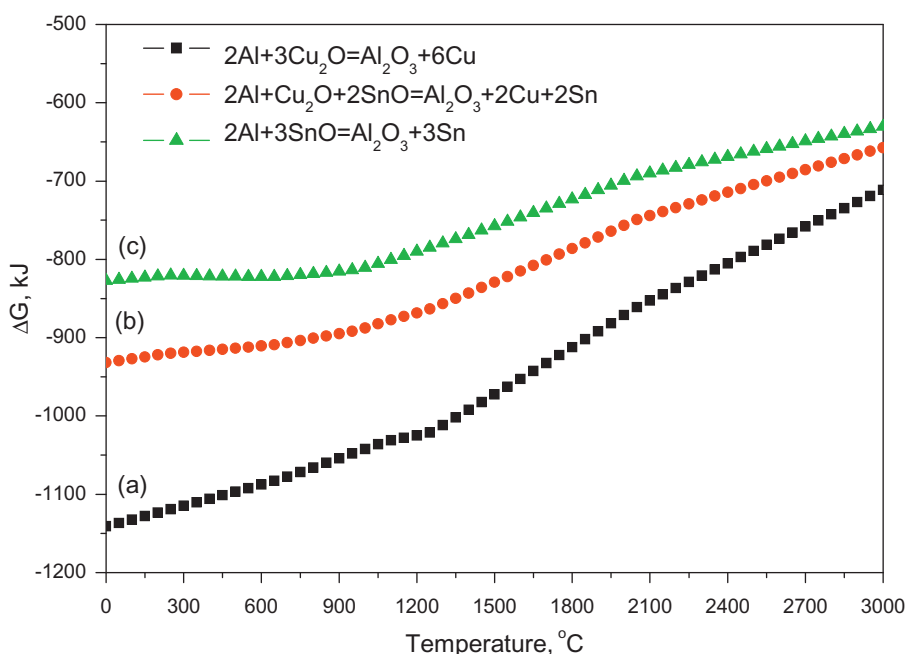
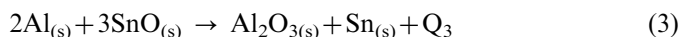
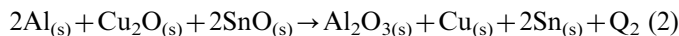
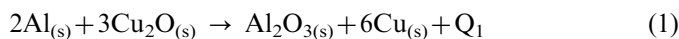


Fig. 2. Gibbs free energies for different aluminothermic reactions in the SnO – Cu_2O –Al system.

3. Calculation

In the SnO–Cu₂O–Al system, the main possible chemical reaction processes were



The Gibbs free energies of the reactions calculated in temperatures from 0 to 3000 °C were plotted in Fig. 2. The aluminothermic reaction (1) occurred more easily than reactions (2) and (3). When the molar ratio of Al, Cu₂O and SnO was 2:1:2, SnO₂ fibers, Al₂O₃ and copper–tin alloy were obtained in the experiments. In this case, once the combustion reaction is triggered, the temperature increases rapidly to the maximum. Al was generated in the reaction, melted and vaporized partially. Molten Al reacted with the nearby Cu₂O and SnO powder to produce Sn gas. At the same time, Sn_(g) also reacted with the surrounding O₂ to form SnO₂ in gas phase:



Combustion synthesis is a technique in which the reaction is maintained by the heat energy produced during the combustion reaction [26,27]. Once the reaction starts with an ignition process, a large amount of heat is produced in several seconds and the reaction temperature is clearly higher than the melting points of Sn (231 °C), Al (660 °C) and Cu (1083 °C). The generated metal Cu and Sn would melt and vaporize after being heated. The combustion products Cu–Sn alloy and Al₂O₃ were in a superheated liquid state at this temperature. Since liquid Al₂O₃ is immiscible with liquid Cu–Sn alloy, it is lifted automatically to the top due to its low density and the Cu–Sn alloy is deposited at the bottom of the crucible as shown in Fig. 3. The SEM image of the marked place in Fig. 3 is shown in Fig. 4. In order to identify the composition of the samples, the EDS analysis was performed on the surface of the samples and the result is inset in the right top corner of Fig. 4(a). Because of the low melting point (231 °C) and boiling point (2260 °C) of Sn, a great deal of tin will be oxidized after vaporizing and SnO₂ will be formed and the molten Cu will precipitate onto the bottom of the crucible.

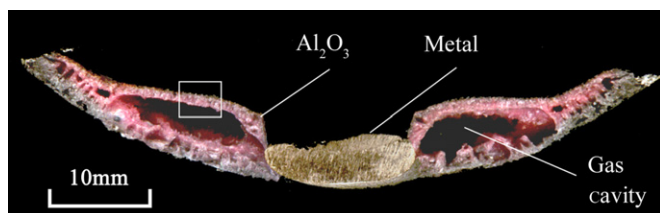


Fig. 3. Optical micrograph of the deposited products of combustion synthesis.

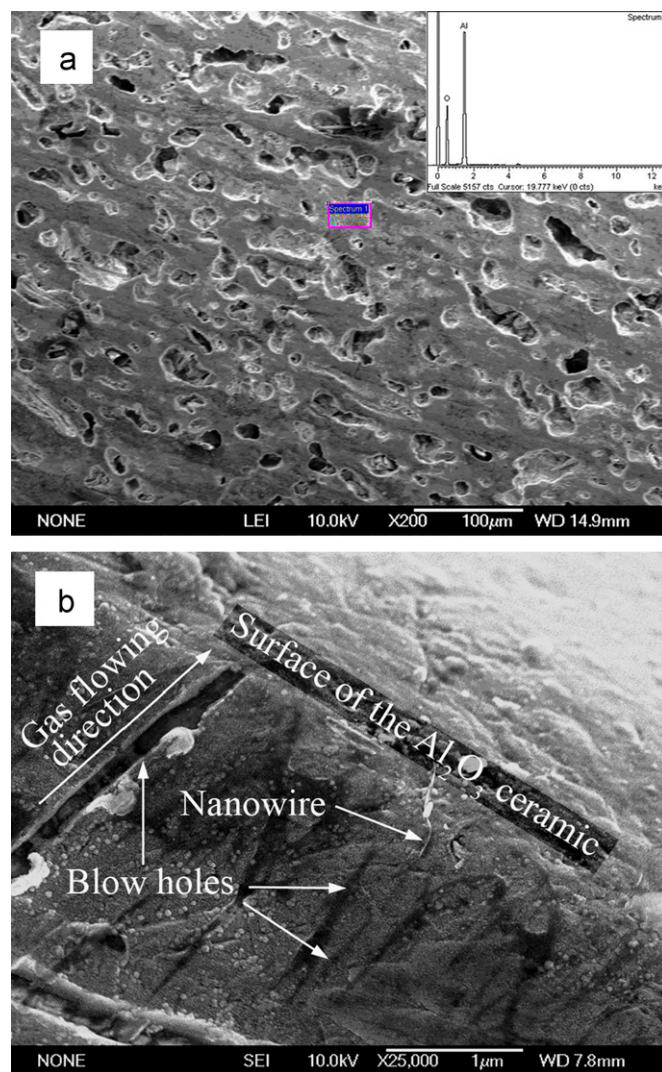


Fig. 4. (a) SEM of porous Al₂O₃ products and (b) its partial enlarge detail.

The loose appearance of SnO₂ can be attributed to the liberation of a large amount of gases during combustion [28].

4. Results and discussion

4.1. Characterization of as-synthesized products

The ignition and combustion synthesis processes were observed through a silica window. When the ignition time reached about 200 s, a combustion initiation reaction with blazing white light emission occurred and a lot of smoke was generated. The combustion initiation reaction may be attributed to the reaction between air and the powders, which might provide an addition of energy to raise the temperature of the reactants up to ignition point. The combustion reaction was completed in a few minutes and the ejected products were collected on the collector sieves. A typical XRD pattern of the as-prepared product is shown in Fig. 5(a). It is clear that the three strongest peaks of SnO₂ at $2\theta = 26.6^\circ$, 33.8° and 51.6° are assigned to

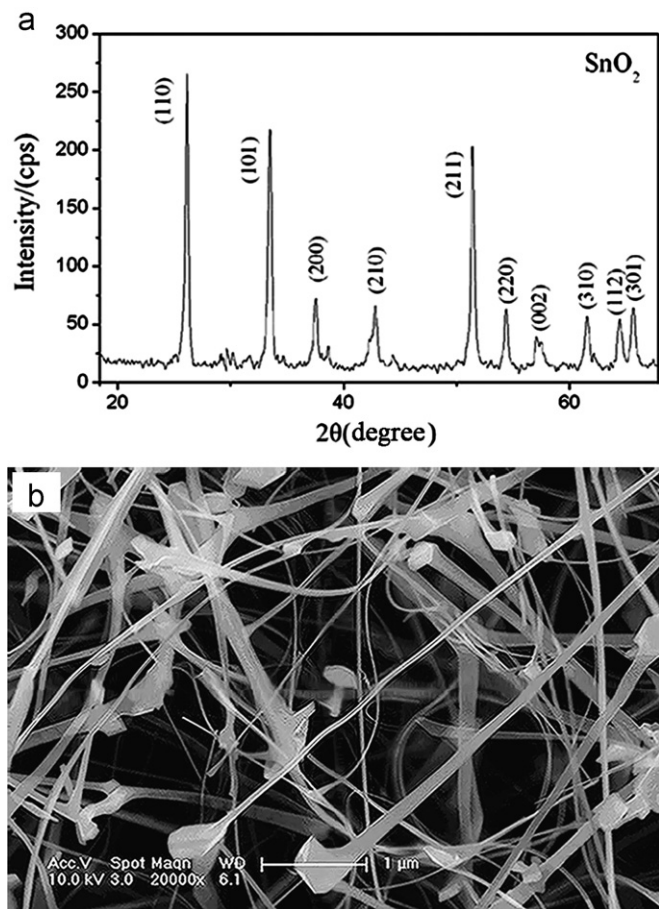


Fig. 5. (a) XRD patterns and (b) SEM of as-prepared by combustion synthesis.

(110), (101) and (211) diffraction peaks of rutile SnO₂, respectively, which indicated that SnO₂ can be prepared by the method of combustion synthesis. Fig. 5(b) shows the FE-SEM image of the as-prepared SnO₂ product, which exhibits fibrous morphology. The SnO₂ fibers are randomly distributed and uniform along the axes with diameters in nanometer magnitude and several micrometers in length.

Detailed microstructures of the SnO₂ nanowires were further investigated by using TEM and HRTEM with the SAED pattern. As shown in Fig. 6, the nanowires have a smooth and uniform surface and the average diameter of the tin oxide nanowires is about 50 nm, which agrees with the SEM observations. The selected area electron diffraction (SAED) pattern collected from the fiber was presented in the upper left corner of Fig. 6(b). The SAED pattern showed that the SnO₂ nanowires were single crystalline with rutile tetragonal crystal structures. The HRTEM image of a single SnO₂ nanowire is shown in Fig. 6(b), which indicates that the crystal has developed perfectly and no dislocations were visible. The interplanar distance (*d*-space) with a diameter of 13 nm in the fiber in Fig. 6(b) was measured to be 0.3333 nm, which is consistent with the *d*-spacing of the (110) planes of rutile SnO₂, indicating that the growth direction of the nanowires is [310].

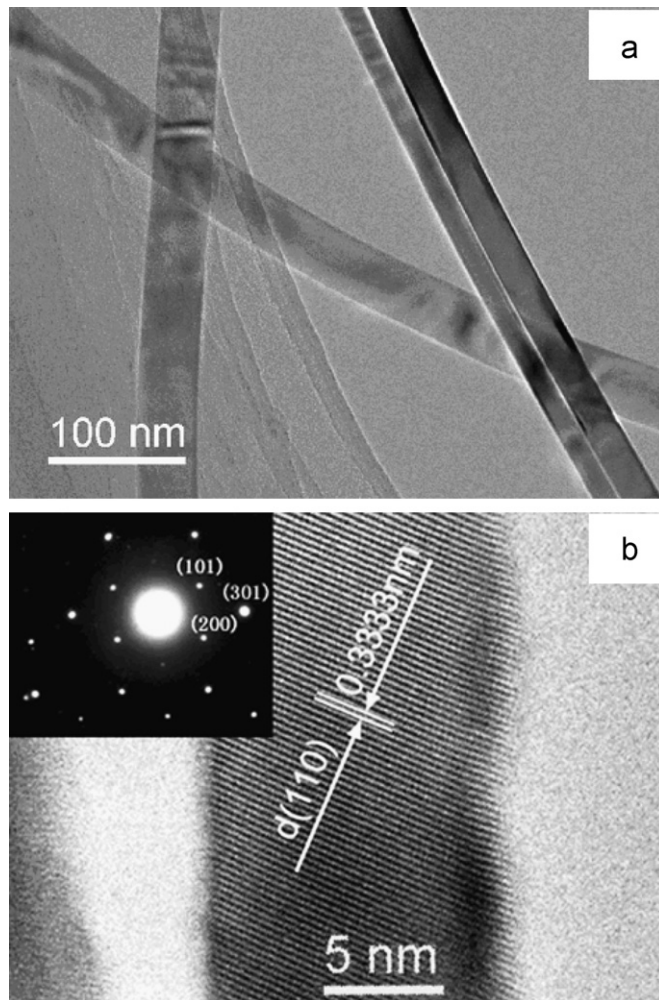


Fig. 6. (a) TEM image and (b) HRTEM image and SAED pattern of SnO₂ nanowires.

4.2. Formation mechanism of SnO₂ nanowires

In general, the growth of fiber is performed via vapor–solid (VS) or vapor–liquid–solid (VLS) mechanisms [26,29]. In the VLS mechanism, a liquid droplet will be initially formed, and then the reactant molecules in the vapor are transported and precipitated on the droplet, after which the crystal grows into a fiber. The fibers formed by VLS are characterized with a round droplet on the head while fibers formed by VS were observed to be without the droplet. In the experiments, both whiskers were observed, which proved that the SnO₂ fibers were formed by both mechanisms. In the combustion synthesis process, once the combustion reaction occurred, the reactants were transformed into products. Meanwhile, the generated metallic Cu and Sn can melt, vaporize, and even boil to generate Sn vapor at the evaluated temperature. The evaporation of the melt will make some dioxide form and also exist in the state of vapor. Since the melt was in superheated liquid state, minor fine Al₂O₃ particles were also entrapped in the vapor in small amounts; these Al₂O₃ particles can act as heterogeneous nucleating sites, and

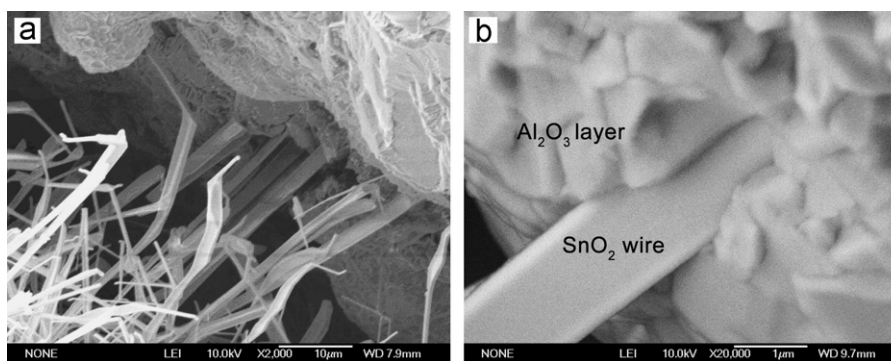
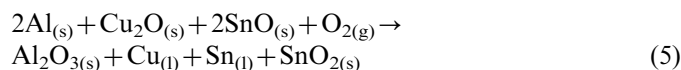


Fig. 7. (a) SEM of quenching sample for combustion synthesis and (b) its partial enlarge detail.

lead to the enhanced nucleation rate [30]. In this case, once a liquid droplet is formed on the surface of as-existed Al_2O_3 crystal, the tin oxide molecules or atoms in vapor phase will dissolve into a liquid and create a supersaturated SnO_2 liquid phase, from which SnO_2 crystals can precipitate. With the continuous precipitation process, the liquid droplet is detached from the substrate surface and SnO_2 nanowires are formed. Combining the above reactions, the formation of the SnO_2 nanowires via the VLS and VS mechanisms could be described as follows:



In the combustion synthesis process, some tin or tin oxide vapor volatilized through the outside reaction product layers (Al_2O_3) and porous ceramics were obtained (Fig. 4). As shown in Fig. 4, the optical micrograph and SEM photomicrograph exhibit the gas flow and fiber trace, which generated the high porous morphologies of the combustion synthesis product. Then SnO_2 is produced via a gas phase reaction between O_2 and Sn vapor. Its nucleation and subsequent growth lead to the formation of nanowire morphology. The combustion synthesis process and fiber growth process were confirmed via the quench technique during the proceeding, and their micrographs were shown in Fig. 7. The outwards material SnO_2 nanowires scattered from the burning substrate Al_2O_3 because of the relatively high pressure gas or vapor release during the reaction.

5. Conclusions

An inexpensive and convenient method was developed to fabricate single crystalline SnO_2 nanowires in the $\text{Al-Cu}_2\text{O-SnO}$ system. The SnO_2 nanowires were obtained by using Al, Cu_2O and SnO as the starting materials with the mole ratio of 2:1:2. The growth mechanism of the SnO_2 nanowires was investigated and three step modes were observed: tin vapor evaporated from the combustion reaction; tin dioxide was formed via a gas phase reaction between O_2 and Sn vapor; and its nucleation and subsequent growth led to the formation of fiber via vapor–solid (VS) and vapor–liquid–solid (VLS) mechanisms. It was

proved by TEM results that the preferred growth direction was [310]. At the same time, porous Al_2O_3 ceramics and Cu–Sn alloy can be obtained during the combustion reaction.

Acknowledgments

This work was supported by the Hebei Natural Science Foundation of China (Grant no. E2011506001) and the National Natural Science Foundation of China (no. 51172281).

References

- [1] X. Song, L. Liu, Characterization of electrospun ZnO-SnO_2 nanowires for ethanol sensor, *Sensors and Actuators A: Physical* 154 (2009) 175–179.
- [2] Y. Shimizu, S. Kai, Y. Takao, T. Hyodo, M. Egashira, Correlation between methylmercaptan gas-sensing properties and its surface chemistry of SnO_2 -based sensor materials, *Sensors and Actuators B:Chemical* 65 (2000) 349–357.
- [3] Q. Qi, T. Zhang, L. Liu, X. Zheng, Synthesis and toluene sensing properties of SnO_2 nanowires, *Sensors and Actuators B:Chemical* 137 (2009) 471–475.
- [4] M. Matsuguchi, T. Uno, T. Aoki, M. Yoshida, Chemically modified copolymer coatings for mass-sensitive toluene vapor sensors, *Sensors and Actuators B:Chemical* 131 (2008) 652–659.
- [5] K. Galatsis, Y.X. Li, W. Wlodarski, E. Comini, G. Sberveglieri, C. Cantalini, S. Santucci, M. Passacantando, Comparison of single and binary oxide MoO_3 , TiO_2 and WO_3 sol–gel gas sensors, *Sensors and Actuators B:Chemical* 83 (2002) 276–280.
- [6] G. Korotcenkov, I. Boris, V. Brinzari, V. Golovanov, Yu. Lychkovsky, G. Karkotsky, A. Cornet, E. Rossinyol, J. Rodrigue, A. Cirera, Gas-sensing characteristics of one-electrode gas sensors based on doped In_2O_3 ceramics, *Sensors and Actuators B:Chemical* 103 (2004) 13–22.
- [7] Y. Lv, Ch. Li, L. Guo, F. Wang, Y. Xu, X. Chu, Triethylamine gas sensor based on ZnO nanorods prepared by a simple solution route, *Sensors and Actuators B:Chemical* 141 (2009) 85–88.
- [8] H. Xu, X. Liu, D. Cui, M. Li, M. Jiang, A novel method for improving the performance of ZnO gas sensors, *Sensors and Actuators B:Chemical* 114 (2006) 301–307.
- [9] D. Wang, X. Chu, M. Gong, Gas-sensing properties of sensors based on single-crystalline SnO_2 nanorods prepared by a simple molten-salt method, *Sensors and Actuators B:Chemical* 117 (2006) 183–187.
- [10] A.Y. El-Etre, S.M. Reda, Characterization of nanocrystalline SnO_2 thin film fabricated by electrodeposition method for dye-sensitized solar cell application, *Applied Surface Science* 256 (2010) 6601–6606.

- [11] Y.P. Yadava, G. Denicoló, A.C. Arias, L.S. Roman, I.A. Hümmelgen, Preparation and characterization of transparent conducting tin oxide thin film electrodes by chemical vapor deposition from reactive thermal evaporation of SnCl_2 , *Materials Chemistry and Physics* 48 (1997) 263–267.
- [12] J. Lee, S. Sim, B. Min, K. Cho, S.W. Kim, S.J. Kim, Structural and optoelectronic properties of SnO_2 nanowires synthesized from ball-milled SnO_2 powders, *Journal of Crystal Growth* 267 (2004) 145–149.
- [13] I.T. Weber, A. Valentini, L.F.D. Probst, E. Longo, E.R. Leite, Catalytic activity of nanometric pure and rare earth-doped SnO_2 samples, *Materials Letters* 62 (2008) 1677–1680.
- [14] Y. Wang, M. Guo, M. Zhang, X. Wang, Facile synthesis of SnO_2 nanograin array films by hydrothermal method, *Thin Solid Films* 518 (2010) 5098–5103.
- [15] Zh. Wang, L. Liu, Synthesis and ethanol sensing properties of Fe-doped SnO_2 nanowires, *Materials Letters* 63 (2009) 917–919.
- [16] Y.C. Lee, H. Huang, O.K. Tan, M.S. Tse, Semiconductor gas sensor based on Pd-doped SnO_2 nanorod thin films, *Sensors and Actuators B:Chemical* 132 (2008) 239–242.
- [17] N. Yang, J. Wang, Y. Guo, X. Zhou, SnO_2 nanowires prepared by sol–gel template method, *Rare Metal Materials and Engineering* 37 (2008) 694–696.
- [18] X. Hou, Z. Yu, Z. Chen, B. Zhao, K. Chou, Single crystalline β - SiAlON nanowhiskers: preparation and enhanced properties at high temperature, *Dalton Transactions* 41 (2012) 7127–7133.
- [19] X. Huang, Z. Liu, Y. Zheng, Q. Nie, Synthesis of SnO_2 nanorods from aqueous solution: the effect of preparation conditions on the formed patterns, *Chinese Chemical Letters* 21 (2010) 999–1002.
- [20] W. Wu, G. Zhang, Y. Kan, P. Wang, Combustion synthesis of ZrB_2 – SiC composite powders ignited in air, *Materials Letters* 63 (2009) 1422–1424.
- [21] A. Morancas, F. Louvet, D.S. Smith, J. Bonnet, High porosity SiC ceramics prepared via a process involving an SHS stage, *Journal of the European Ceramic Society* 23 (2003) 1949–1956.
- [22] J. Li, Z. Cai, H. Guo, B. Xu, L. Li, Characteristics of porous Al_2O_3 – TiB_2 ceramics fabricated by the combustion synthesis, *Journal of Alloys and Compounds* 479 (2009) 803–806.
- [23] U. Anselmi-Tamburini, G. Chiodelli, M. Arimondi, F. Maglia, G. Spinolo, Z.A. Munir, Electrical properties of Ni/YSZ cermets obtained through combustion synthesis, *Solid State Ionics* 110 (1998) 35–43.
- [24] H.E. Çamurlu, F. Maglia, Preparation of nano-size ZrB_2 powder by self-propagating high-temperature synthesis, *Journal of the European Ceramic Society* 29 (2009) 1501–1506.
- [25] G. Liu, K. Chen, H. Zhou, K. Ren, J. Li, C. Pereira, J.M.F. Ferreira, Formation of β - SiAlON micropalings consisting of nanorods during combustion synthesis, *Scripta Materialia* 55 (2006) 935–938.
- [26] G. Liu, K. Chen, H. Zhou, X. Ning, C. Pereira, J.M.F. Ferreira, Preparation of Ca α - SiAlON powders with rod-like crystals by combustion synthesis, *Ceramics International* 32 (2006) 411–416.
- [27] W. Wang, Zh. Fu, H. Wang, R. Yuan, Chemistry reaction processes during combustion synthesis of B_2O_3 – TiO_2 – Mg system, *Journal of Materials Processing Technology* 128 (2002) 162–168.
- [28] Ch. Lin, Ch. Hwang, W. Lee, W. Tong, Preparation of zinc oxide (ZnO) powders with different types of morphology by a combustion synthesis method, *Materials Science and Engineering B* 140 (2007) 31–37.
- [29] R.S. Wagner, W.C. Ellis, Vapor–liquid–solid mechanism of single crystal growth, *Applied Physics Letters* 4 (1964) 89–90.
- [30] L. Li, Q. Bi, J. Yang, W. Liu, Q. Xue, Fabrication of bulk Al_2O_3 dispersed ultrafine-grained Cu matrix composite by self-propagating high-temperature synthesis casting route, *Materials Letters* 62 (2008) 2458–2460.